

MicroRNA-139-3p suppresses growth and metastasis of glioblastoma via inhibition of NIN1/RPNI2 binding protein 1 homolog

L. SHI¹, Y. YUAN², H.-Y. LI¹

¹Department of Neurosurgery, Dezhou People's Hospital, Dezhou, Shandong, China

²Department of Neurosurgery, Yantai Yuhuangding Hospital, Yantai, Shandong, China

Lin Shi and Yuan Yuan contributed equally to this work

Abstract. – **OBJECTIVE:** This study aimed to investigate the role of microRNA-139-3p (miR-139-3p) in glioblastoma, and further explored the underlying molecular mechanism.

PATIENTS AND METHODS: Gene Expression Omnibus (GEO) dataset (accession code GSE90603) was selected to identify differentially expressed microRNAs in glioblastoma. The level of miR-139-3p in glioblastoma tissues and cell lines was detected by quantitative Real Time-Polymerase Chain Reaction (qRT-PCR). 3-(4,5-dimethylthiazol-2-yl)-2,5-diphenyl tetrazolium bromide (MTT), colony formation, wound healing, and transwell invasion assays were applied to assess the role of miR-139-3p in glioblastoma cells growth and aggressiveness. The direct target of miR-139-3p was confirmed using luciferase reporter assay. NIN1/RPNI2 binding protein 1 homolog (NOB1), specific short hairpin RNA (shRNA), and lentiviral vector encoding NOB1 stable transfections were done. The expression levels of NOB1 were detected by Western blotting and qRT-PCR. Glioblastoma cells were subcutaneously implanted into nude mice to determine the role of miR-139-3p in tumor growth and metastasis *in vivo*.

RESULTS: miR-139-3p was remarkably down-expressed in glioblastoma tissue compared to control normal tissue. Overexpression of miR-139-3p suppressed the growth and metastasis of glioblastoma cells. Moreover, miR-139-3p inhibited glioblastoma growth and lung metastasis *in vivo*, whereas under-expression of miR-139-3p caused an opposite outcome. Furthermore, our work revealed that NOB1 expression was negatively associated with miR-139-3p, and NOB1 knock-down mimicked the inhibitory effect of miR-139-3p on glioblastoma cell proliferation and mobility phenotypes. Finally, overexpression of NOB1 neutralized the inhibition of miR-139-3p in glioblastoma cells.

CONCLUSIONS: Our findings indicated that miR-139-3p played a vital role in inhibiting glioblastoma growth and metastasis by targeting NOB1.

Key Words:

Glioblastoma, MiR-139-3p, Growth, Metastasis.

List of abbreviations

GEO, gene expression omnibus; NOB1, NIN1/RPNI2 binding protein 1 homolog; qRT-PCR, quantitative real-time polymerase chain reaction; MTT, 3-(4,5-dimethylthiazol-2-yl)-2,5-diphenyl tetrazolium bromide; shRNA, short hairpin RNA; GBM, glioblastoma; FBS, fetal bovine serum; DMEM, Dulbecco modified Eagle's medium; TMZ, temozolomide; DMSO, dimethyl sulfoxide; WT, wild-type; MUT, mutant-type; OD, optical density; GAPDH, glyceraldehyde-3-phosphate dehydrogenase; 3'-UTR, 3'-untranslated region, cDNA, complementary DNA; NSCLC, non-small cell lung cancer; TNM, tumor-node-metastatic.

Introduction

Glioma is a frequently occurring type of primary malignant cancer of the human brain¹. The current therapeutic methods include maximal resection, followed by radiotherapy in combination with temozolomide (TMZ)². Glioblastoma (GBM) is the most aggressive type of glioma and exhibits strong aggression properties³. The invasive phenotype is critical to the clinical progression of malignant GBM, and complicates complete surgical resection and permits postoperative tumor re-growth⁴. Therefore, there is an urgent need for the development of novel mechanistic methods to investigate the invasiveness and migration properties of cancer cells, which could be exploited to design more effective therapeutic strategies.

MicroRNAs are small non-coding RNAs that post-transcriptionally control the expression of their down-stream target genes⁵. Substantive

studies demonstrate that altered expression of microRNA is related to human cancer progression, including growth, metastasis, angiogenesis, and chemotherapy resistance⁶. MicroRNAs commonly function as tumor suppressors or oncogenes and play vital roles in the diagnosis and treatment of cancer⁷. Previous researches have identified abnormal microRNA expression to be closely associated with the prognosis of patients across several cancers⁸. MiR-139-3p is markedly lower in patients with colorectal cancer than in control subjects and is a potential non-invasive biomarker for detection of colorectal cancer⁹. Furthermore, miR-139-3p acts as a tumor suppressor that restricts cervical cancer cell growth and aggressiveness, and induces cell apoptosis via inhibition of NIN1/RPNI2 binding protein 1 homolog (NOB1)¹⁰. NOB1 is a subunit of the 26 S proteasome, encoding a 50-kDa protein and contains a zinc ribbon domain and a PIN domain¹¹. Wang et al¹² identified that NOB1 is up-regulated in epithelial cancers, including prostate, hepatocellular carcinoma, lung, and pancreatic cancers, and that down-regulation of NOB1 restrains growth and mobility in renal cancer cells. In addition, down-regulation of NOB1 inhibits the growth and cell colony formation ability of ovarian cancer cells. However, how abnormal miR-139-3p expression regulates glioblastoma invasion and metastasis, has not yet been fully investigated.

In this investigation, we demonstrated that miR-139-3p was remarkably down-regulated in glioblastoma samples, including clinical specimens and cell lines. With overexpression of miR-139-3p, cellular growth, invasion, and metastasis were significantly inhibited, and the same effect was observed on tumor growth *in vivo*, whereas down-expression of miR-139-3p resulted in completely opposite outcomes. In addition, we demonstrated that NOB1, a miR-139-3p target gene, played a very important role in this process.

Materials and Methods

Glioblastoma Specimens and Cell Lines

Forty frozen paraffin-embedded specimens (35 human glioblastoma samples and 5 para-tumor tissue samples) were obtained from Binzhou Central Hospital. Informed consents of patients were obtained before surgery. The glioblastoma cell lines (U251, U-87MG, SHG-

44, and TJ905) and normal human brain glial cells, HEB, were obtained from the Cobioer Biotechnology Co., Ltd (Nanjing, Jiangsu, China). The cell lines were cultured in RPMI-1640 or Dulbecco Modified Eagle's Medium (DMEM) supplemented with 10% fetal bovine serum (FBS) (Wisent, Quebec, Canada), with 100 U/mL penicillin and 100 µg/mL streptomycin.

Transfection of MiR-139-3p Precursors and Inhibitor

MiR-139-3p mimic (named as miR-139-3p) and its positive control mimic (named as miR-NC), as well as miR-139-3p inhibitor (miR-139-3p^{inhi}) and its negative control (miR-NC^{inhi}), were provided by Ambion (GeneCopoeia, Guangzhou, Guangdong, China). Transfection of miR-139-3p or inhibitors was carried out using Lipofectamine RNAiMAX transfection reagent (Invitrogen, Carlsbad, CA, USA)¹³.

Transient Transfection and Lentiviral Constructs

Transfection of vectors or short hairpin RNA (shRNA) was conducted with Lipofectamine 2000 (Invitrogen, Carlsbad, CA, USA). The shRNA against NOB1 was designed and purchased from Genepharma Co., Ltd (Shanghai, China). Lentiviral vector encoding NOB1 complementary DNA (cDNA) was constructed by Genepharma Co., Ltd (Shanghai, China) and designated as pLV-NOB1. The empty vector was used as control (pLV-vector).

Luciferase Reporter Assay

293T cells were seeded in a 96-well plate at 70 to 80 % confluence. After 24 h, the cells were transfected with miR-139-3p and wild-type (WT) or mutant-type (MUT) 3'-UTR of NOB1 gene. Forty-eight hours after transfection, the cells were collected and Renilla luciferase activity was assessed by using a dual-luciferase reporter system (Promega, Madison, WI, USA)¹⁴.

Cell Proliferation Assay

Cells were plated into 96-well plates, and cultured for 1, 2, or 3 days. 5 mg/ml 3-(4,5-dimethylthiazol-2-yl)-2,5-diphenyl tetrazolium bromide (MTT) was added into 96-well plates. After 4 h, the supernatant was removed and 200 µl dimethyl sulfoxide (DMSO) was added; the optical density (OD) value was determined at 490 nm¹⁵.

Wound Healing Assay

Cells were seeded into a 6-well plate. After 24 h, the monolayer cells were created by using a 100 μ l tip, and cells were continually cultured with serum-free medium. The wound closure at 0 h and 24 h was photographed, and the percentage of the wound closure was calculated¹⁶.

Transwell Invasion Assay

Cells were seeded into a Matrigel-coated chamber (8 μ m), and placed in a 24-well plate. After 24 h, the lower chamber cells were fixed and stained with 0.1% crystal violet. The invading cells were counted¹⁷.

Colony Formation Assay

Cells were cultured in a 25-mm³ dish and placed in an incubator for four weeks. The colonies were stained with 0.1% crystal violet and the number of cell colonies was calculated¹⁸.

Quantitative Real-time RT-PCR (qRT-PCR) Assay

Total RNA was isolated using Trizol (TaKaRa, Otsu, Shiga, Japan). RNA (1 μ g) was reverse-transcribed to cDNA using a PrimeScript RT reagent kit (TaKaRa, Otsu, Shiga, Japan). qRT-PCR was performed to detect the level of miR-139-3p or other genes using IQTM SYBR Green Supermix and Bio-Rad iQ5 real-time detection system. The formula for the relative expression value was through $2^{(-\Delta\Delta C_t)}$ method¹⁹. The reference gene, U6 was used while detecting the level of miR-139-3p in glioblastoma tissues and para-tumor tissues. The primers used for PCR were as follows: GAPDH, (forward primer): 5'-CTGGGCTACTGAGCACC-3' and (reverse primer): 5'-AAGTGGTCGTTGAGGGCAATG-3'; NOB1, (forward primer): 5'-TGTTAAACCCCTAAAGGGAGACC-3' and (reverse primer): 5'-CCTTGTCGGTGTCACATTCTCT-3'

Western Blotting

Total proteins were collected in RIPA Lysis Buffer containing protein inhibitors (Beyotime, Guangzhou, Guangdong, China). Membranes were incubated with anti-NOB1 or anti-GAPDH (1:1000, Abcam, Cambridge, MA, USA) at 4°C overnight and hybridized with horseradish peroxidase-conjugated goat anti-rabbit IgG antibody. Target proteins were assessed by using the enhanced chemiluminescence (ECL) system (Millipore, Braunschweig, Germany) and visual-

ized with the ChemiDoc XRS system (Bio-Rad, Hercules, CA, USA)²⁰.

Xenograft Model of Glioblastoma In Vivo

All nude mice were bred and housed in AAA-LAC-accredited SPF rodent facilities at the People's Hospital of Dezhou City. All experiments were approved by the Animal Ethics Committee of the People's Hospital of Dezhou City. MiR-139-3p or miR-NC transfected cells were subcutaneously injected into the flanks of nude mice. The tumor sizes were measured each week²¹, and calculated as tumor volume = length \times width²/2. To study metastasis *in vivo*, glioblastoma cells were transfected with miR-139-3p or miR-139-3p inhibitor and injected into tail vein of nude mice. After six weeks, the mice were sacrificed and the lungs were excised. The lungs were stained with Bouin's solution for 24 h and then paraffin-embedded, sectioned, and stained with hematoxylin and eosin staining (H&E)²².

Statistical Analysis

Results are presented as Mean \pm SD for three repeated experiments and the difference was compared using the Student's *t*-test. $p < 0.05$ was considered statistically significant.

Results

MiR-139-3p is Down-Expressed in Glioblastoma

Gene expression datasets used for statistical analysis were acquired from the GEO database with the accession code GSE90603. The screening was performed in GEO datasets that contained both the glioblastoma samples and the matched normal tissues samples. As shown in Figure 1A, miR-139-3p was down-expressed in glioblastoma samples as compared to that in control samples. In order to compare miR-139-3p expression pattern in glioblastoma and control tissue, miR-139-3p levels were evaluated in 35 glioblastoma tissues and 5 para-tumor tissues. As shown in Figure 1B, miR-139-3p level in glioblastoma was significantly lower than that in the control tissues. MiR-139-3p levels were also determined in a panel of glioblastoma cell lines by qRT-PCR. Similar results were obtained in four glioblastoma cell lines, in which the levels of miR-139-3p were lower compared to those in normal human brain glial cells, HEB (Figure 1C). In order to investigate the role of miR-139-3p

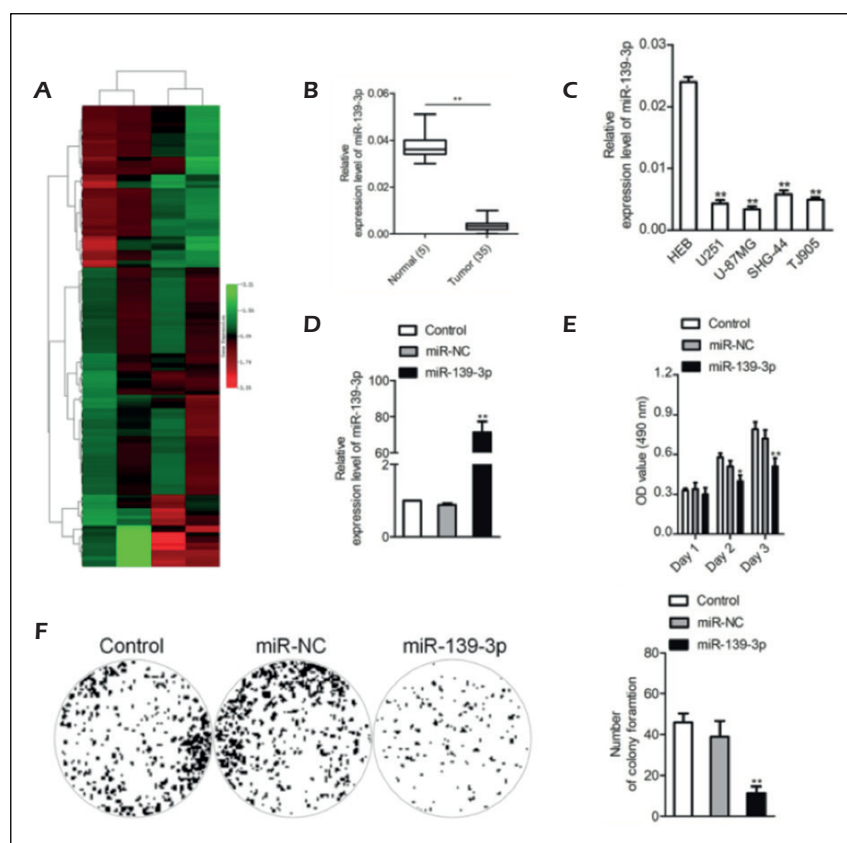


Figure 1. MiR-139-3p inhibits glioblastoma cells growth. **A**, Microarray analysis of miRNA expression in glioblastoma tissues and corresponding normal tissues. **B**, The level of miR-139-3p from the normal tissues and tumor tissues of patients with glioblastoma was determined by qRT-PCR assay. $**p < 0.01$, compared to normal. **C**, MiR-139-3p levels were measured in five different glioblastoma cell lines by qRT-PCR. $**p < 0.01$, compared to HEB cells. **D**, U-87MG cells were transfected with miR-NC or miR-139-3p. The level of miR-139-3p was determined by qRT-PCR. **E**, Cells were plated into 96-well plates and cultured for 1, 2 or 3 days. MTT assay was performed and OD value was measured at 490 nm. **F**, Cells were subjected to soft agar colony formation assay in a 6-well culture plate. The cell colonies were counted after four weeks. Data are presented as the mean \pm SD from three independent measurements. $**p < 0.01$, compared to control.

in the growth of glioblastoma, we constructed the miR-139-3p overexpression system. MiR-139-3p was significantly up-regulated in miR-139-3p transfected glioblastoma U-87MG cells (Figure 1D). The MTT assay results showed that the induction of miR-139-3p significantly inhibited the proliferation of glioblastoma cells (Figure 1E). Colony formation growth analysis revealed that miR-139-3p overexpression inhibited the colony growth of tumor cells (Figure 1F). These observations suggest that miR-139-3p is a tumor suppressor in glioblastoma.

MiR-139-3p Overexpression Inhibits Cell Migration and Invasion

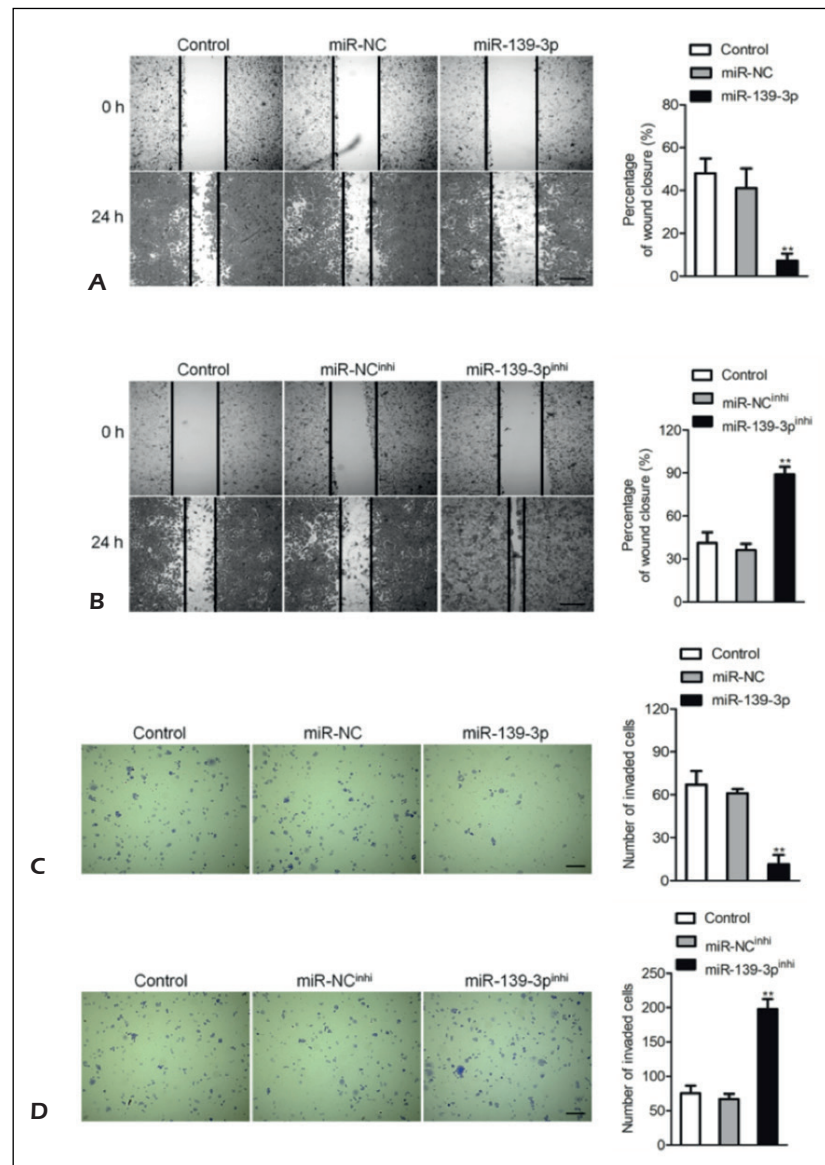
To demonstrate the effect of miR-139-3p on migration, we performed wound closure assays, whereby we observed that the distance between wound edges in miR-139-3p-transfected U-87MG cells was markedly longer than that in control cells (Figure 2A). Additionally, we observed shorter distance in the wound edges of miR-139-3p^{inhi}-transfected U-87MG cells compared with that in control (Figure 2B). To investigate the effect of altered miR-139-3p expression on glioblas-

toma cell invasion, we performed the transwell analysis, wherein we observed that miR-139-3p overexpression remarkably suppressed U-87MG cell invasion (Figure 2C). We found that miR-139-3p^{inhi} significantly accelerated glioblastoma cell invasion *in vitro* (Figure 2D).

MiR-139-3p Overexpression Inhibits Glioblastoma Cell Metastasis *in vivo*

In vitro, miR-139-3p markedly inhibited glioblastoma cell growth, migration, and invasion. Whether miR-139-3p regulated tumor growth and metastasis *in vivo* was needed to be further investigated. MiR-139-3p transfected U-87MG cells were subcutaneously implanted into the nude mice. Tumors were monitored and measured every week. MiR-139-3p overexpression remarkably inhibited growth and tumor volume of glioblastoma cells (Figure 3A). We dissected the mice to harvest the tumor, noting that the Ki67 staining was remarkably inhibited in miR-139-3p group than in the miR-NC group (Figure 3B), which confirmed that miR-139-3p inhibited glioblastoma growth *in vivo*. In addition, the occurrence of lung metastasis of glioblastoma cells in the

Figure 2. Effects of miR-139-3p on aggressiveness in glioblastoma cells. **A**, Wound healing analysis of U-87MG cells. A representative image was shown (*left panel*). Histograms showed the percentage of wound closure (*right panel*). **B**, Transwell analysis. A representative image was shown (*left panel*). Histograms showed the number of invaded cells (*right panel*). **C**, Wound healing analysis of U-87MG cells. A representative image was presented (*left panel*). Histograms exhibited the percentage of wound closure (*right panel*). **D**, Transwell assay. Photographs show cells that invaded through the membrane (*left panel*). A representative image was shown (*left panel*). Histograms showed the number of invaded cells (*right panel*). ** $p < 0.01$, compared to control.



miR-139-3p transfection group was remarkably suppressed, as compared to that in control group (Figure 3C). All these results showed that miR-139-3p inhibits the growth and metastasis of glioblastoma cells *in vivo*.

miR-139-3p Directly Binds to the 3'-UTR of NOB1

Generally, microRNAs regulate their target genes by binding to their 3'-UTR regions²³. miR-Base and TargetScan were selected to predict the targets of miR-139-3p and we found that NOB1 may be a target of miR-139-3p (Figure 4A). To investigate whether miR-139-3p binds directly to the 3'-UTR of NOB1 and modulates NOB1 expres-

sion, 3'-UTR of NOB1 was cloned into the downstream of the luciferase reporter gene. Reduced luciferase activity revealed that NOB1 is indeed a target of miR-139-3p (Figure 4B). Taken together, the results indicated that miR-139-3p regulated NOB1 by binding to the 3'-UTR region directly. QRT-PCR assay analysis showed that glioblastoma cell lines exhibited high NOB1 expression as compared to the normal human brain glial cells, HEB (Figure 4C). In addition, NOB1 showed higher expression in glioblastoma samples compared to that in normal tissue samples (Figure 4D). We also investigated the relationship between miR-139-3p and NOB1 in glioblastoma specimens. As shown in Figure 4E, there was a negative correlation

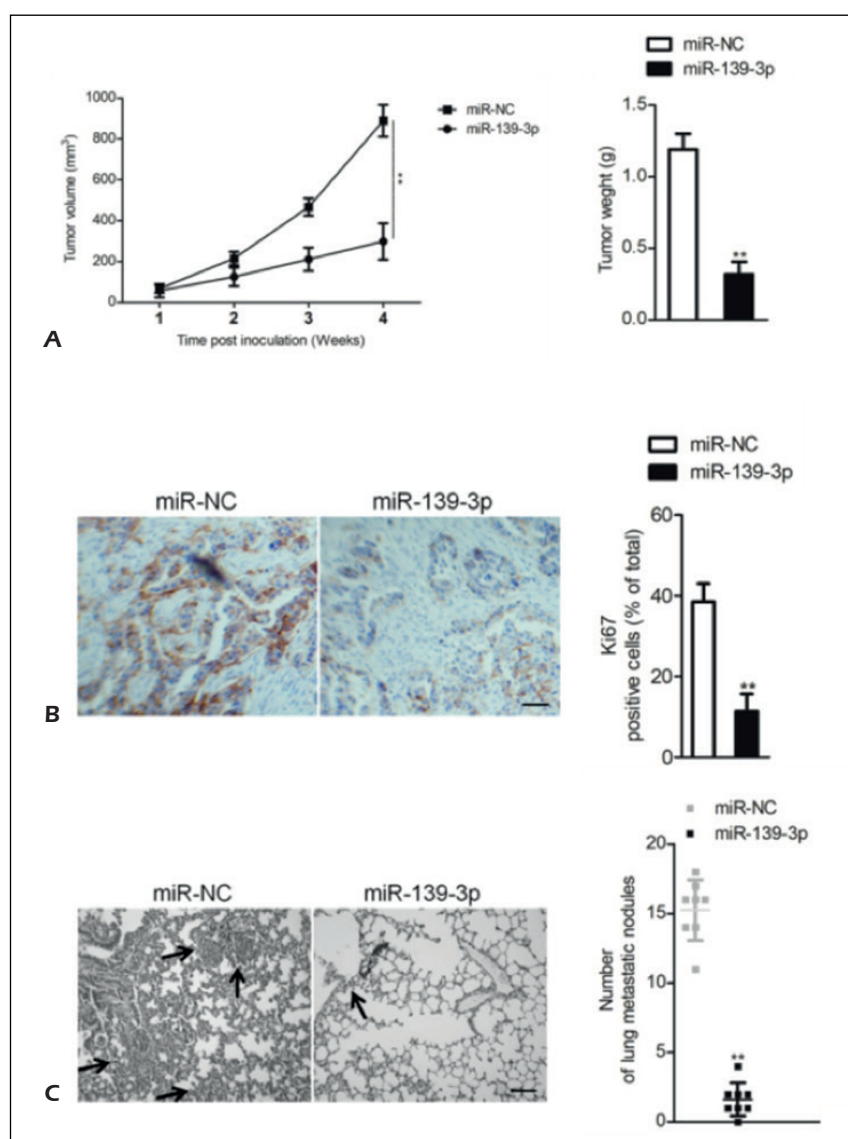


Figure 3. Effect of miR-139-3p on glioblastoma cells tumor growth and metastasis *in vivo*. **A**, MiR-NC or miR-139-3p U-87MG cells were implanted into the nude mice. Measure the tumor volume each week. **B**, Tumor we removed and embedded in paraffin for immunohistochemical staining with Ki67. **C**, Metastatic lesions in the lungs of the glioblastoma cells metastasis models were shown after 6 weeks. The numbers of metastatic lung lesions in the miR-139-3p transfection groups were much less than those in miR-NC group. ** $p < 0.01$, compared to miR-NC group.

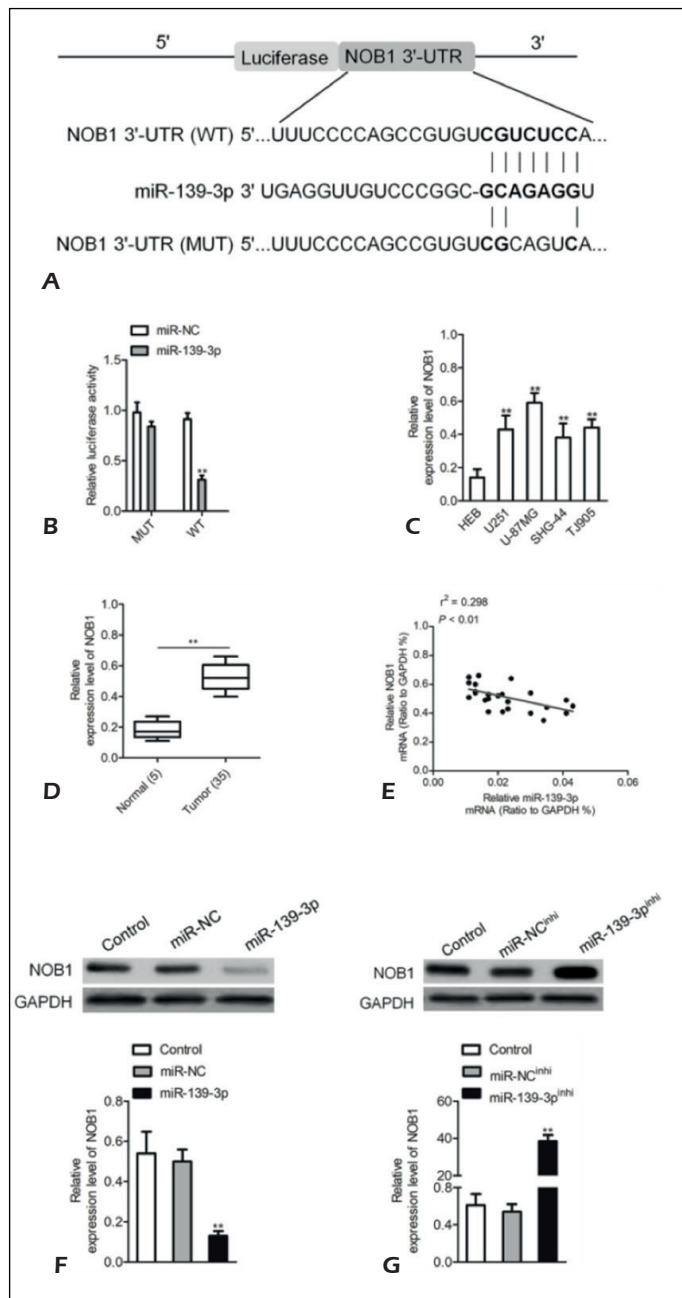
between miR-139-3p levels and NOB1 levels. Additionally, NOB1 was significantly down-regulated after U-87MG was transfected with miR-139-3p (Figure 4F), whereas NOB1 was remarkably up-regulated after transfection with miR-139-3p^{inhi} (Figure 4G). These observations hint that NOB1 may be a target gene of miR-139-3p.

The Effect of MiR-139-3p on Glioblastoma is Rescued by NOB1 Overexpression

Little is known about the role of NOB1 in glioblastoma progression, and whether NOB1 knock-down could mimic the effect of miR-139-3p in glioblastoma. Short hairpin RNA (shRNA), specifically targeting NOB1 (shNOB1), was used

to stably knock down the expression of NOB1 in the U-87MG cells (Figure 5A). To determine the role of NOB1 in glioblastoma growth and metastasis, the effect of NOB1 knock-down on U-87MG cell proliferation, colony formation, migration and invasion was examined (Figure 5B-5E). The stable knock-down of NOB1 in U-87MG had a similar effect as miR-139-3p overexpression on the growth, migration and invasion of U-87MG cells *in vitro*, which suggested that NOB1 might play an oncogenic role by promoting glioblastoma growth and metastasis. To investigate whether miR-139-3p suppresses the growth and mobility of glioblastoma cells by inhibiting NOB1, we constructed a U-87MG cell line that was transfected with miR-139-3p

Figure 4. NOB1 is the target of miR-139-3p. **A**, Predicted miR-139-3p target sequences in 3'-UTR of NOB1. **B**, Luciferase activity of NOB1 (MT or MUT) was evaluated after miR-139-3p transfection into 293T cells. $**p < 0.01$, compared to miR-NC. **C**, The expression level of NOB1 was detected by qRT-PCR assay in several glioblastoma cell lines. $**p < 0.01$, compared to HEB cells. **D**, The level of NOB1 in glioblastoma tissues was measured by qRT-PCR. $**p < 0.01$, compared to normal. **E**, The correlation analysis of miR-139-3p and NOB1 expressions. **F**, The level of NOB1 in U-87MG cells after cells transfected with miR-139-3p was measured by qRT-PCR and Western blotting assays. **G**, The expression level of NOB1 in U-87MG cells after cells transfected with miR-139-3pinhi was measured by qRT-PCR and Western blot analysis. $**p < 0.01$, compared to control.



and pLV-NOB1. Immunoblotting and qRT-PCR analysis demonstrated that ectopic expression of NOB1 rescued its expression after U-87MG cells were transfected with miR-139-3p (Figure 6A). MTT assay, colony formation, wound closure and transwell assay exhibited that NOB1 overexpression restored the inhibition of miR-139-3p in glioblastoma cell growth and metastasis (Figure 6B-6E). Altogether, these results demonstrated that miR-139-3p inhibits cell growth and metastasis of glioblastoma by targeting NOB1.

Discussion

Glioblastoma is one of the most aggressive tumors, and the occurrence of metastasis leads to a sharp decline in the survival rate of patients²⁴. Thus, identification of metastasis-related biomarkers and therapeutic targets will help improve glioblastoma prognosis. There is increasing evidence to suggest that miRNAs have vital roles in tumor progression in controlling their target genes, and thus they might serve as biomarkers

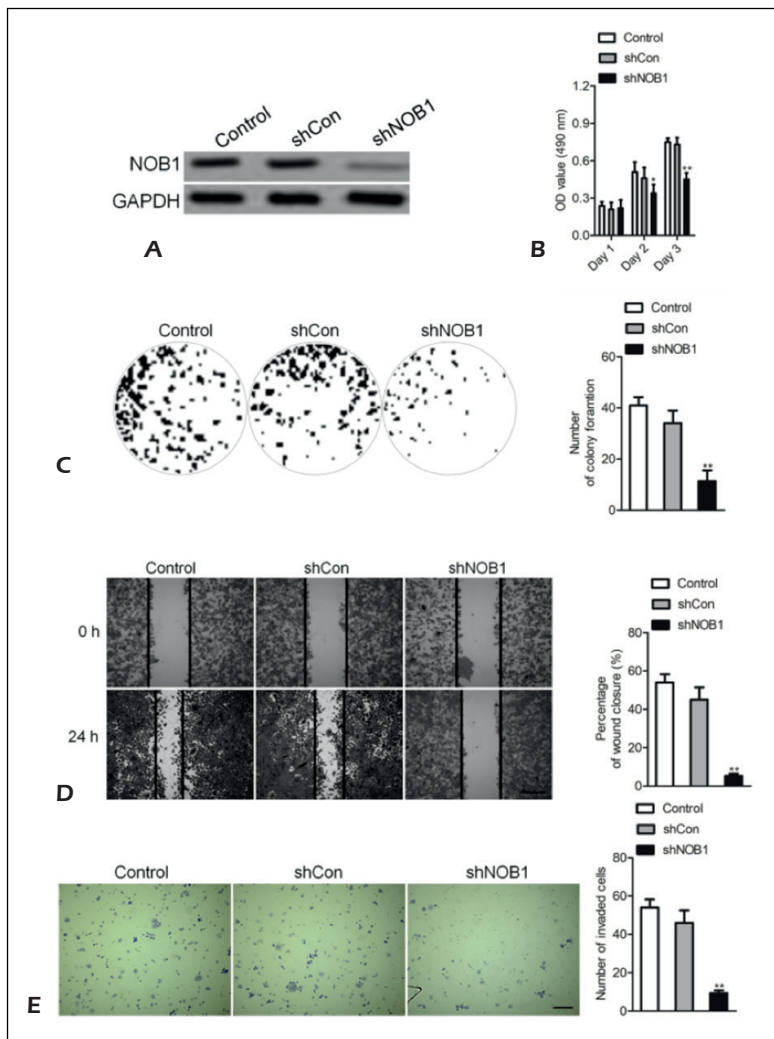


Figure 5. NOB1 knock-down mimics the effects of miR-139-3p on U-87MG cells. **A**, To knock-down NOB1, shNOB1 or shCon were transfected into U-87MG cells. The NOB1 was detected by Western blot. **B**, U-87MG cells proliferation activity was measured by MTT. **C**, Colony formation ability of U-87MG cells was measured by the soft agar colony formation assay. The image and quantitative analysis of colonies were shown. **D**, U-87MG cells were transfected with shNOB1 or shCon, and then the migration ability of the cells was investigated with the wound healing assay. Quantitative analysis of the percentage of wound closure from three independent experiments was shown. **E**, The invasion capacity of U-87MG cells was investigated with the transwell invasion assay. Quantitative analysis of the invasive cells was shown. The data are presented as mean \pm SD. * p <0.05, ** p <0.01, compared to control.

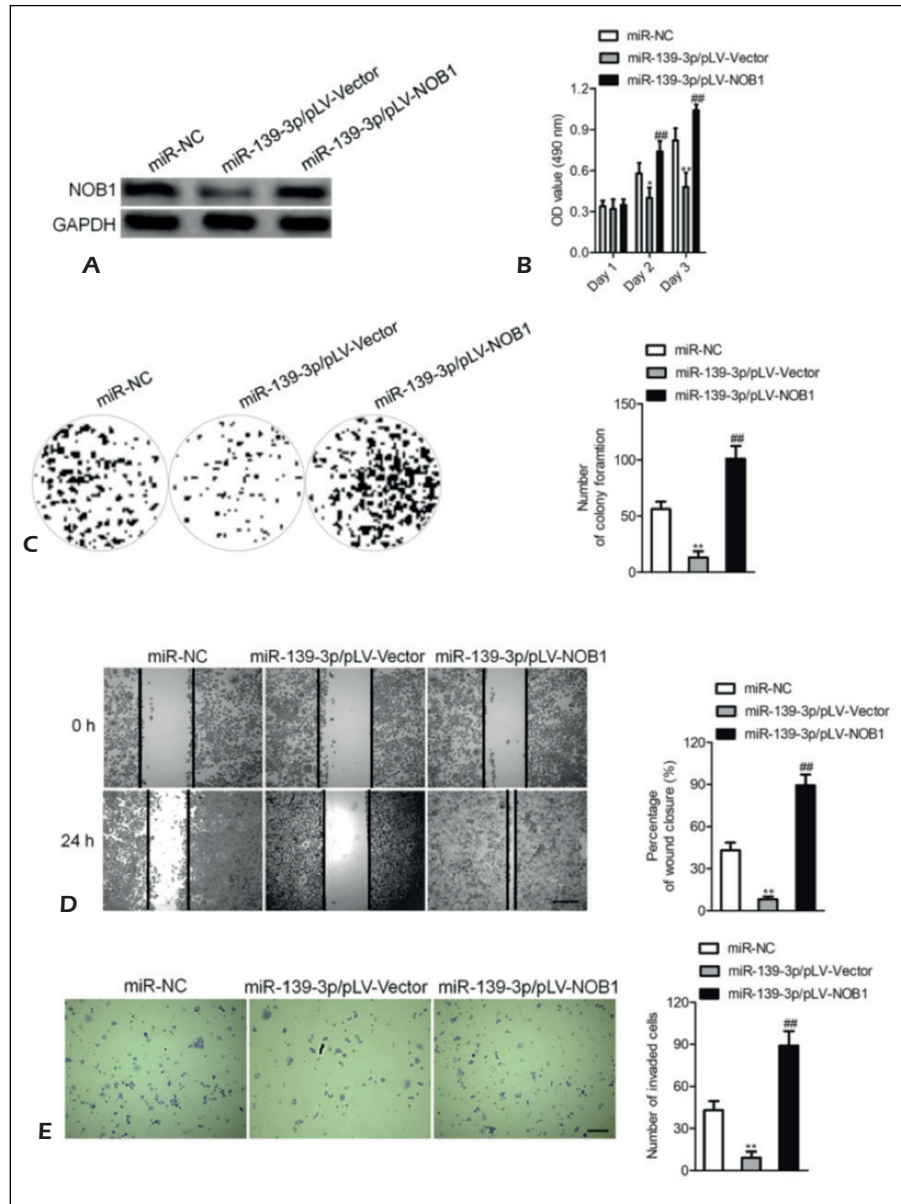
for prediction and prognosis of cancers²⁵. Here, we report that miR-139-3p is a novel metastasis-associated miRNA that plays a significant role in regulating glioblastoma growth and metastasis. We found a significant decrease in miR-139-3p levels in glioblastoma and miR-139-3p was found to prevent glioblastoma cell proliferation and progression by inhibiting NOB1 expression.

NOB1 is frequently expressed in the liver, lung, and spleen, and is mainly located in the nucleus. It was reported that NOB1 is abnormally expressed in invasive ductal carcinoma and may be involved in the occurrence and development of tumors²⁶. The expression of NOB1 messenger RNA (mRNA) and proteins in papillary thyroid carcinoma is significantly higher than that in normal thyroid tissues²⁷. In non-small cell lung cancer (NSCLC) and prostate cancer, the NOB1 expression is correlated with tumor-node-metastatic (TNM) stages and lymph node

metastasis²⁸. Consistently, our results verified that NOB1 level was markedly increased in glioblastoma compared to controls.

In addition, the use of shRNA knock-down of NOB1 inhibits U-87MG cell growth, migration, and invasion, suggesting that NOB1 plays a crucial role in regulating glioblastoma cell proliferation and metastasis. It is acknowledged that miRNAs regulate gene expression by binding to the 3'-UTR of the target genes. In this study, a bioinformatics approach was used to predict NOB1 as a candidate target gene and luciferase reporter assay was performed, for *in vitro* confirmation. Meanwhile, the expression of NOB1 was down-regulated and up-regulated in U-87MG cells after transfection with miR-139-3p and miR-139-3p^{inhi}, respectively. In addition, overexpression of NOB1 neutralized the effects of miR-139-3p suppression. These results corrob-

Figure 6. Effect of miR-139-3p on glioblastoma cells rescues by NOB1 overexpression. **A**, pLV-NOB1 was transfected into U-87MG. The expression level of NOB1 was detected by Western blot. **B**, Cell proliferation activity was measured by MTT assay. **C**, Growth ability was measured by the colony formation assay *in vitro*. The image and quantitative analysis of colonies were shown. **D**, U-87MG cells were co-transfected with pLV-NOB1 and miR-139-3p, and then the migration ability of the cells was investigated with the wound healing assay. **E**, The invasion ability of the cells was investigated with the transwell invasion assay. The data are presented as mean \pm SD. * $p < 0.05$, ** $p < 0.01$, compared to miR-NC. ## $p < 0.01$, compared to cell co-transfected with miR-139-3p and pLV-Vector.



orate that miR-139-3p act as a tumor suppressor by inhibiting NOB1 in glioblastoma progression.

Conclusions

We observed the down-regulation of miR-139-3p in glioblastoma. Overexpression of miR-139-3p inhibited the growth, invasion, and metastasis of glioblastoma, whereas inhibition of miR-139-3p resulted in almost the opposite outcomes. NOB1, the direct target gene of miR-139-3p, plays a crucial role in this process. These findings may help us to investigate the mechanism of miR-

139-3p regulation of glioblastoma better, and might provide a novel therapeutic target for the treatment of glioblastoma growth and metastasis.

Conflict of Interests

The authors declare that no conflicts of interest exist.

References

- 1) MANN J, RAMAKRISHNA R, MAGGE R, WERNICKE AG. Advances in radiotherapy for glioblastoma. *Front Neurol* 2017; 8: 748.

- 2) DU C, REN J, ZHANG R, XIN T, LI Z, ZHANG Z, XU X, PANG Q. Effect of bevacizumab plus temozolomide-radiotherapy for newly diagnosed glioblastoma with different MGMT methylation status: a meta-analysis of clinical trials. *Med Sci Monit* 2016; 22: 3486-3492.
- 3) FANG DZ, WANG YP, LIU J, HUI XB, WANG XD, CHEN X, LIU D. MicroRNA-129-3p suppresses tumor growth by targeting E2F5 in glioblastoma. *Eur Rev Med Pharmacol Sci* 2018; 22: 1044-1050.
- 4) BREDEL M, BREDEL C, JURIC D, HARSH GR, VOGEL H, RECHT LD, SIKIC BI. Functional network analysis reveals extended gliomagenesis pathway maps and three novel MYC-interacting genes in human gliomas. *Cancer Res* 2005; 65: 8679-8689.
- 5) ZAPOROZHCHENKO IA, MOROZKIN ES, SKVORTSOVA TE, PONOMARYOVA AA, RYKOVA EY, CHERDYNTSEVA NV, POLOVNIKOV ES, PASHKOVSKAYA OA, POKUSHALOV EA, VLASSOV VV, LAKTIONOV PP. Plasma miR-19b and miR-183 as potential biomarkers of lung cancer. *PLoS One* 2016; 11: e0165261.
- 6) BENTINK S, HAIBE-KAINS B, RISCH T, FAN JB, HIRSCH MS, HOLTON K, RUBIO R, APRIL C, CHEN J, WICKHAM-GARCIA E, LIU J, CULHANE A, DRAPKIN R, QUACKENBUSH J, MATULONIS UA. Angiogenic mRNA and microRNA gene expression signature predicts a novel subtype of serous ovarian cancer. *PLoS One* 2012; 7: e30269.
- 7) ESLAMIZADEH S, HEIDARI M, AGAH S, FAGHIHLOO E, GHAZI H, MIRZAEI A, AKBARI A. The role of microRNA signature as diagnostic biomarkers in different clinical stages of colorectal cancer. *Cell J* 2018; 20: 220-230.
- 8) BRAGA EA, LOGINOV VI, BURDENNYI AM, FILIPPOVA EA, PRONINA IV, KUREVLEV SV, KAZUBSKAYA TP, KUSHLINSKII DN, UTKIN DO, ERMILOVA VD, KUSHLINSKII NE. Five hypermethylated microRNA genes as potential markers of ovarian cancer. *Bull Exp Biol Med* 2018; 164: 351-355.
- 9) ZHANG L, DONG Y, ZHU N, TSOI H, ZHAO Z, WU CW, WANG K, ZHENG S, NG SS, CHAN FK, SUNG JJ, YU J. microRNA-139-5p exerts tumor suppressor function by targeting NOTCH1 in colorectal cancer. *Mol Cancer* 2014; 13: 124.
- 10) HUANG P, XI J, LIU S. MiR-139-3p induces cell apoptosis and inhibits metastasis of cervical cancer by targeting NOB1. *Biomed Pharmacother* 2016; 83: 850-856.
- 11) VEITH T, MARTIN R, WURM JP, WEIS BL, DUCHARDT-FERNER E, SAFFERTHAL C, HENNIG R, MIRUS O, BOHNSACK MT, WOHNERT J, SCHLEIFF E. Structural and functional analysis of the archaeal endonuclease Nob1. *Nucleic Acids Res* 2012; 40: 3259-3274.
- 12) WANG J, CAO L, WU J, WANG Q. Long non-coding RNA SNHG1 regulates NOB1 expression by sponging miR-326 and promotes tumorigenesis in osteosarcoma. *Int J Oncol* 2018; 52: 77-88.
- 13) JONES DZ, SCHMIDT ML, SUMAN S, HOBGING KR, BARVE SS, GOBEJISHVILI L, BROCK G, KLINGE CM, RAI SN, PARK J, CLARK GJ, AGARWAL R, KIDD LR. MicroRNA-186-5p inhibition attenuates proliferation, anchorage independent growth and invasion in metastatic prostate cancer cells. *BMC Cancer* 2018; 18: 421.
- 14) ZHOU L, ZHAO LC, JIANG N, WANG XL, ZHOU XN, LUO XL, REN J. MicroRNA miR-590-5p inhibits breast cancer cell stemness and metastasis by targeting SOX2. *Eur Rev Med Pharmacol Sci* 2017; 21: 87-94.
- 15) BLOCKHUYS S, VANHOECKE B, SMET J, DE PAEPE B, VAN COSTER R, BRACKE M, DE WAGTER C. Unraveling the mechanisms behind the enhanced MTT conversion by irradiated breast cancer cells. *Radiat Res* 2013; 179: 433-443.
- 16) YANG Z, JI L, JIANG G, LIU R, LIU Z, YANG Y, MA Q, ZHAO H. FL118, a novel camptothecin analogue, suppressed migration and invasion of human breast cancer cells by inhibiting epithelial-mesenchymal transition via the Wnt/beta-catenin signaling pathway. *Biosci Trends* 2018; 12: 40-46.
- 17) TOMIDA C, YAMAGISHI N, NAGANO H, UCHIDA T, OHNO A, HIRASAKA K, NIKAWA T, TESHIMA-KONDO S. VEGF pathway-targeting drugs induce evasive adaptation by activation of neuropilin-1/cMet in colon cancer cells. *Int J Oncol* 2018; 52: 1350-1362.
- 18) SALIMI R, BANDARU S, DEVARAKONDA S, GOKALP S, ALA C, ALVANDIAN A, YENER N, AKYUREK LM. Blocking the cleavage of filamin a by calpain inhibitor decreases tumor cell growth. *Anticancer Res* 2018; 38: 2079-2085.
- 19) SOOTICHOTE R, THUWAJIT P, SINGSUKSAWAT E, WARNNISORN M, YENCHITSOMANUS PT, ITHIMAKIN S, CHANTHARASAMEE J, THUWAJIT C. Compound A attenuates toll-like receptor 4-mediated paclitaxel resistance in breast cancer and melanoma through suppression of IL-8. *BMC Cancer* 2018; 18: 231.
- 20) CHENG ZX, SONG YX, WANG ZY, WANG Y, DONG Y. miR-144-3p serves as a tumor suppressor by targeting FZD7 and predicts the prognosis of human glioblastoma. *Eur Rev Med Pharmacol Sci* 2017; 21: 4079-4086.
- 21) ESPOSITO CL, NUZZO S, CATUOGNO S, ROMANO S, DE NIGRIS F, DE FRANCISCIS V. STAT3 Gene silencing by Aptamer-siRNA chimera as selective therapeutic for glioblastoma. *Mol Ther Nucleic Acids* 2018; 10: 398-411.
- 22) MURAKAMI K, WU Y, IMAIZUMI T, AOKI Y, LIU Q, YAN X, SEINO H, YOSHIZAWA T, MOROHASHI S, KATO Y, KIJIMA H. DEC1 promotes hypoxia-induced epithelial-mesenchymal transition (EMT) in human hepatocellular carcinoma cells. *Biomed Res* 2017; 38: 221-227.
- 23) LIU Z, WANG C, JIAO X, ZHAO S, LIU X, WANG Y, ZHANG J. miR-221 promotes growth and invasion of hepatocellular carcinoma cells by constitutive activation of NFkappaB. *Am J Transl Res* 2016; 8: 4764-4777.
- 24) CHOWDHURY FA, HOSSAIN MK, MOSTOFA AGM, AKBOR MM, BIN SAYEED MS. Therapeutic potential of thymoquinone in glioblastoma treatment: targeting major gliomagenesis signaling pathways. *Biomed Res Int* 2018; 2018: 4010629.
- 25) ORSO F, QUIRICO L, VIRGA F, PENNA E, DETTORI D, CIMINO D, COPPO R, GRASSI E, ELIA AR, BRUSA D, DEAGLIO S, BRIZZI MF, STADLER MB, PROVERO P, CASELLE M, TAVERNA D. miR-214 and miR-148b targeting inhibits dissemination of melanoma and breast cancer. *Cancer Res* 2016; 76: 5151-5162.

- 26) LI XY, LUO QF, LI J, WEI CK, KONG XJ, ZHANG JF, FANG L. Clinical significance of NOB1 expression in breast infiltrating ductal carcinoma. *Int J Clin Exp Pathol* 2013; 6: 2137-2144.
- 27) LIU J, DONG BF, WANG PS, REN PY, XUE S, ZHANG X, HAN Z, CHEN G. Silencing NOB1 enhances doxorubicin antitumor activity of the papillary thyroid carcinoma *in vitro* and *in vivo*. *Oncol Rep* 2015; 33: 1551-1559.
- 28) LI Y, MA C, QIAN M, WEN Z, JING H, QIAN D. Down-regulation of NOB1 suppresses the proliferation and tumor growth of non-small cell lung cancer *in vitro* and *in vivo*. *Oncol Rep* 2014; 31: 1271-1276.